dimension causes a change of 4% in the Curie point and this is a reasonable change in view of the experiments on change of the Curie point by hydrostatic pressure.[12]

[12] K. Werner, Ann. Physik **2**, 403 (1959).

ACKNOWLEDGMENTS

The authors are much indebted to R. Pauthenet and V. C. Morruzi for sending them valuable data prior to publication, and to C. Kittel for valuable discussion of the work.

PHYSICAL REVIEW VOLUME 123, NUMBER 3 AUGUST 1, 1961

Effective X-Ray and Calorimetric Debye Temperature for Copper

P. A. FLINN, G. M. MCMANUS, AND J. A. RAYNE
Westinghouse Research Laboratories, Pittsburgh, Pennsylvania
(Received March 27, 1961)

The Debye-Waller factor for copper was determined from x-ray intensity measurements on a single crystal over the temperature range 4.2°K–500°K. From a machine calculation of the vibrational spectrum of copper the values of the specific heat and Debye-Waller factor were obtained and compared with those found by experiment. The agreement indicates that for copper the central force model with nearest- and second-neighbor interactions is adequate for the interpretation of effects depending on simple averages over the frequency spectrum.

INTRODUCTION

EXPERIMENTAL data on the Debye-Waller factor for x-ray reflections have hitherto been interpreted in terms of the theory for an ideal Debye solid. The general theory for an elastic solid has been available for many years,[1] and has been applied to an analysis of the diffuse scattering[2]; there has been no corresponding analysis of the elastic scattering. Attempts to correlate calorimetric data with x-ray results on the basis of the simple Debye theory have been somewhat inconclusive.

To remedy this situation, we chose copper as a solid whose elastic properties have been extensively investigated down to 4°K, and for which accurate calorimetric data are available over a wide temperature range. We made corresponding x-ray intensity measurements over the temperature range 4.2°–500°K. We also carried out a machine calculation of the vibrational spectrum of copper, and compared the predicted values of specific heat and Debye-Waller factor with those obtained experimentally.

DETAILS

The x-ray measurements were performed on a single crystal of copper grown from the melt by the usual Bridgman technique. A slice was cut so as to expose a (100) face, and was polished electrolytically to remove the cold-worked layer and annealed in vacuum. The crystal was then mounted in the cryostat shown in Fig. 1. The cryostat is constructed of thin-wall stainless steel tubing, with over-all dimensions approximately 15 in. in height and $4\frac{1}{2}$ in. in diameter. The liquid coolant is held in the 250-cc chamber L, surrounded by, successively, a vacuum chamber V, a secondary cooling well K, and again the vacuum chamber V. The specimen chamber S is enclosed by a copper radiation shield with an aluminum foil window. A 10-mil thick beryllium strip soldered onto a semicircumferential slot in the outer wall of the cryostat permits x rays to enter and leave the specimen chamber. Under a good vacuum (10^{-6} mm) the cryostat will hold liquid helium for almost 24 hours.

In order to align the crystal for maximum reflected intensity two degrees of freedom are needed in the specimen mount, which is shown in detail in Fig. 2. The single crystal is clamped on the flat plate M, which is free to rotate in its own plane in a bearing in the cradle C. Similarly, the cradle C is held on bearings in the base mounts B attached to the liquid chamber L. All parts, B, C, and M, are of copper. A screw T pushes against the cradle C so as to tilt the crystal out of the plane of the axis of the cryostat, and a screw R pushes on the mount M to produce a rotation of the crystal in its own plane. For x-ray measurements, the cryostat was mounted on a Berthold spectrometer equipped with a NaI(Tl) scintillation counter. To obtain high-index reflections, we used Mo $K\alpha$ radiation, crystal-monochromated to minimize background. By the method described in a previous paper[3] we measured the integrated intensities of the (600), (800), and (1000) reflections at selected temperatures between 4.2° and 500°K. To correct for the diffuse scattering component of the measured intensity, the diffuse intensity adjacent to the Bragg peaks was extrapolated to the peak region, and this value was subtracted from the observed main

[1] R. W. James, *The Optical Principles of the Diffraction of X-Rays* (G. Bell and Sons, London, 1954), Chap. V.
[2] See, e.g., E. H. Jacobsen, Phys. Rev. **97**, 851 (1954).
[3] P. A. Flinn, G. M. McManus, and J. A. Rayne, J. Phys. Chem. Solids **15**, 189 (1960).

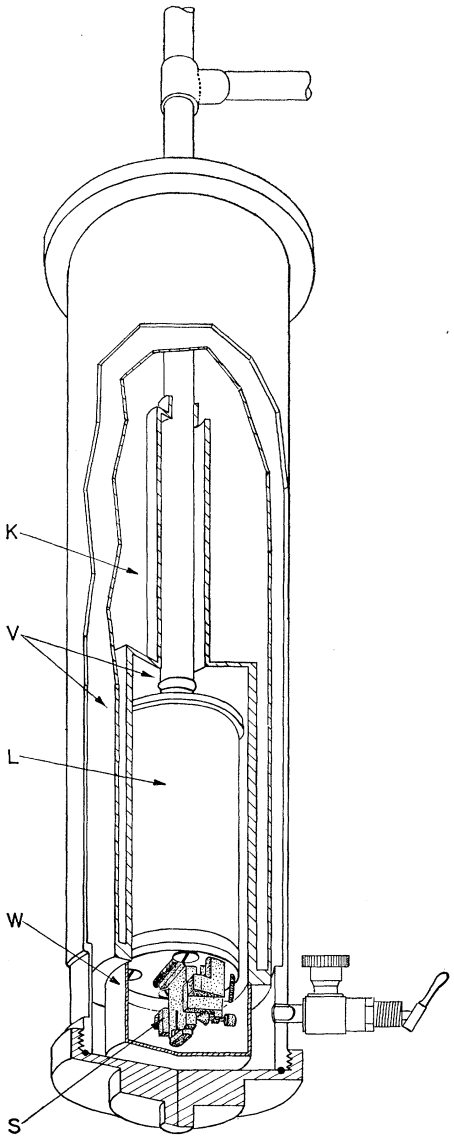

FIG. 1. The liquid helium cryostat.

peak to give the total integrated intensity of the reflection.

For low-temperature intensity measurements we used liquid helium (4.2°K), liquid nitrogen (77°K), and carbon dioxide and acetone (200°K) in the cooling chamber. For room-temperature measurements we placed acetone in the liquid chamber of the cryostat to act as a thermal reservoir. We obtained higher temperatures by using boiling butyl acetate (400°K) and boiling *n*-decyl alcohol (500°K) in the cryostat chamber. An immersion heater maintained the liquid at the boiling point and the vapor refluxed. The high temperatures were stable to ±2°C.

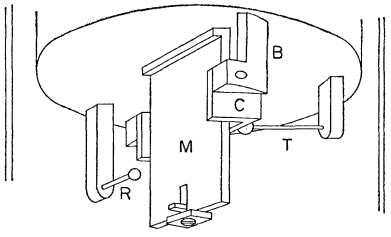

FIG. 2. Detail of the cryostat specimen mount.

EXPERIMENTAL RESULTS

It is convenient to express the observed Debye-Waller factor in terms of an effective Debye Θ. In the Debye approximation, the exponent $2M$ of the Debye-Waller factor is given by

$$2M=\frac{12h^2}{mk\Theta}\left\{\frac{\phi(x)}{x}+\frac{1}{4}\right\}\left(\frac{\sin\theta}{\lambda}\right)^2. \tag{1}$$

Here m is the atomic mass, Θ the Debye temperature, $x=\Theta/T$, and $\phi(x)$ is the Debye function:

$$\phi(x)=\frac{1}{x}\int_0^x \frac{z\,dz}{e^z-1}.$$

This equation will apply to a real solid if Θ is now regarded as temperature dependent and different from the calorimetric Θ, which involves a different average over the vibrational spectrum. The observed intensity is related to the initial intensity J by

$$\ln I=\ln J-\frac{A\sigma^2}{\Theta}\left\{\frac{\phi(x)}{x}+\frac{1}{4}\right\}, \tag{2}$$

where $\sigma=\sin\theta/\lambda$ and A contains only known constants. For each reflection, we can calculate the ratio of the intensities at two temperatures T_0 and T_1:

$$\ln\left(\frac{I_0}{I_1}\right)=-\frac{A\sigma_0^2}{\Theta_0}\left\{\ \right\}+\frac{A\sigma_1^2}{\Theta_1}\left\{\ \right\}. \tag{3}$$

Because of thermal expansion, σ slightly varies with temperature. Equation (3) can be rearranged to give

$$\ln\left(\frac{I_0}{I_1}\right)=-A\left\{\frac{\sigma_0^2\phi(x_0)}{T_0x_0^2}-\frac{\sigma_1^2\phi(x_1)}{T_1x_1^2}+\frac{1}{4}\left(\frac{\sigma_0^2}{T_0x_0}-\frac{\sigma_1^2}{T_1x_1}\right)\right\}. \tag{4}$$

This can be greatly simplified by taking $T_0=4.2$°K, since for $\Theta\sim300$°K the first term of (4) is of the order 10^{-6} and can be ignored. The last term of this equation has the form $(\Theta_1-\Theta_0)/4\Theta_1\Theta_0$ and, except for low temperatures, can be ignored in comparison with the remaining term. Under these restrictions, Eq. (4) as-

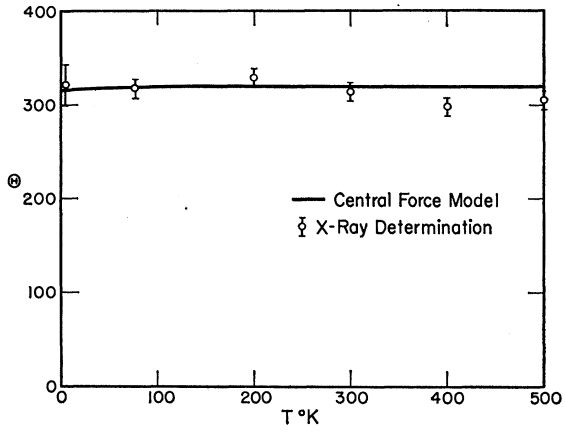

FIG. 3. The calculated and experimental effective x-ray Θ's.

sumes the useful form

$$\ln\left(\frac{I_0}{I_1}\right)=A\sigma_1{}^2\frac{\phi(x_1)}{T_1x_1{}^2}. \tag{5}$$

At each temperature above 100°K we calculated $\ln I_0-\ln I_1$ for the (600), (800), and (1000) reflection and averaged the three values of Θ determined from Eq. (5) to give the final Θ_T for that temperature. The value of Θ_0 was found in the following manner: Knowing the Θ's for $T=200°$, 300°, 400°, and 500°K, the average value of $\ln J$ was calculated for the (600), (800), and (1000) reflections directly from Eq. (2). Using these values and the intensity of each reflection at $T=4.2$°K, Θ_0 was then determined from Eq. (2), giving $\Theta_0=322°\text{K}\pm22°\text{K}$. With this value of Θ_0, the value of Θ_{77} was determined from Eq. (4), using Eq. (5) as a first approximation. These effective values of Θ_T are plotted in Fig. 3. The error estimates shown are based on the scatter in the results from the three reflections measured.

CENTRAL FORCE MODEL CALCULATIONS

A review of the theory of lattice dynamics is given in the article by de Launay,[4] and the information requisite to the calculation of the vibrational spectrum is contained therein. For a face-centered cubic lattice with nearest- and next-nearest neighbor central force interactions, the equations of motion of the Born-von Kármán theory yield the dynamical matrix,

$$\begin{bmatrix} 2+2\beta S_1{}^2-C_1(C_2+C_3) & S_1S_2 & S_1S_3 \\ S_1S_2 & 2+2\beta S_2{}^2-C_2(C_1+C_3) & S_2S_3 \\ S_1S_3 & S_2S_3 & 2+2\beta S_3{}^2-C_3(C_1+C_2) \end{bmatrix}, \tag{6}$$

where $S_i=\sin(\pi aK_i)$, $C_i=\cos(\pi aK_i)$, $\beta=(c_{11}-c_{12}-c_{44})/4c_{44}$, and a is the lattice parameter. The eigenvalues of this matrix are $\rho a^2\omega^2/2c_{44}$, where ρ is the density. The exponent $2M$ is given in terms of the eigenvectors and eigenvalues of the vibrational spectrum by

$$2M=\frac{\hbar}{2mN}\sum_{ij}\frac{1}{\omega_{ij}}(\mathbf{S}\cdot\mathbf{e}_{ij})^2(\bar{n}_{ij}+\tfrac{1}{2}), \tag{7}$$

where $\mathbf{S}=4\pi\sigma$(unit scattering vector); $\mathbf{e}_{ij}$=polarization vector for the ith polarization of the jth lattice mode; ω_{ij}=angular frequency of the i, j lattice mode; and $\bar{n}_{ij}$=average occupation number of the i, j lattice mode.

$$\bar{n}_{ij}=(\exp\xi_{ij}-1)^{-1},$$

where $\xi_{ij}=\hbar\omega_{ij}/kT$.

From consideration of cubic symmetry, it can be shown[5] that the factor $(\mathbf{S}\cdot\mathbf{e}_{ij})^2$ may be replaced by its average value outside the summation, so that Eq. (7) reduces to

$$2M=\frac{8\pi^2\hbar}{3mN}\sigma^2\sum_{ij}\frac{1}{\omega_{ij}}(\bar{n}_{ij}+\tfrac{1}{2}). \tag{8}$$

The specific heat is given by

$$C_v=k\sum_{ij}\xi_{ij}{}^2e^{\xi ij}/(e^{\xi ij}-1)^2. \tag{9}$$

To evaluate these sums, it is necessary to determine the characteristic frequencies at a suitable number of points in an irreducible section (1/48) of the first Brillouin zone. At low temperatures the major contributions to the sums come from low frequencies corresponding to small values of **K**. For this reason we used a smaller mesh near the origin of **K** space. Using the low-temperature values of the elastic constants of copper,[6]

$$c_{11}=1.762\times10^{12}\text{ dyne/cm}^2,$$
$$c_{12}=1.249\times10^{12}\text{ dyne/cm}^2,$$
$$c_{44}=0.818\times10^{12}\text{ dyne/cm}^2,$$

the dynamical matrix was diagonalized by the Jacobi method[7] at about 4000 points in **K** space, and Eqs. (8) and (9) evaluated at 50° intervals between 0° and 500°K. The histogram of the frequency spectrum obtained is shown in Fig. 4. The cutoff frequencies and the critical points are in agreement with analytical predictions.[8] The calculated values of the Debye-Waller factor are given in Table I, and the corresponding effective x-ray Θ's are shown in Fig. 3. From the calculated specific heats, the effective specific heat Θ's were derived and are shown in Fig. 5, along with experimental data, corrected for electronic heat capacity

[4] J. de Launay, in *Solid-State Physics*, edited by F. Seitz and D. Turnbull (Academic Press, New York, 1956), Vol. 2, p. 220.

[5] W. H. Zachariasen, *Theory of X-Ray Diffraction in Crystals* (John Wiley & Sons, Inc., New York, 1945), p. 208.

[6] W. C. Overton and J. Gaffney, Phys. Rev. **98**, 969 (1955).

[7] See P. A. White, J. Soc. Indust. Appl. Math. **6**, 393 (1958).

[8] H. B. Rosenstock, Phys. Rev. **97**, 290 (1955).

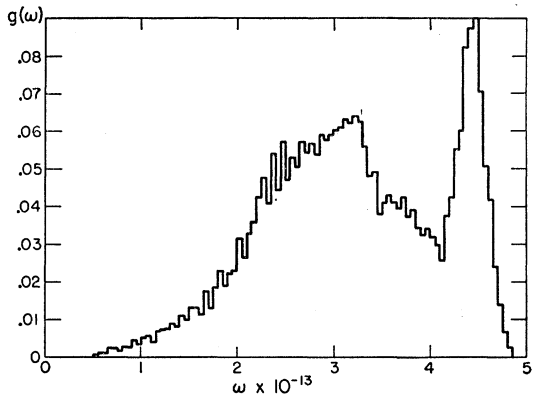

FIG. 4. The frequency spectrum histogram of copper.

and converted to constant volume. The data up to 300°K are from Giauque and Meads,[9] and above 300°K from Bronson.[10]

DISCUSSION

It is clear from Figs. 3 and 5 that the central force model with nearest- and second-neighbor interactions is adequate for the interpretation of effects depending on averages over the frequency spectrum. We do not believe that the discrepancy between theory and experiment for the calorimetric Θ in the temperature range 200°–300°K is significant. The accuracy of the data in this range is low, and the discrepancy is of the order of the discontinuity between two sets of data. Effects such as inelastic scattering which depend on the fine details of the frequency spectrum are known to require a more sophisticated approach involving more complicated interatomic force laws.[11] It is notable that both our experimental and theoretical results for the x-ray Θ fail to show the marked temperature dependence noted by other observers.[12] In addition, over most of the temperature range, the x-ray effective Θ is quite close to the calorimetric Θ, rather than substantially higher, as predicted from a simple argument based on a modified Debye model.[1] We have made no correction for lattice expansion or other anharmonic effects in this work, since no adequate theory for such effects on either specific heat or x-ray scattering is presently available. It appears that it is not necessary to invoke anharmonic effects to obtain agreement between theory and experiment at the present level of experimental accuracy.

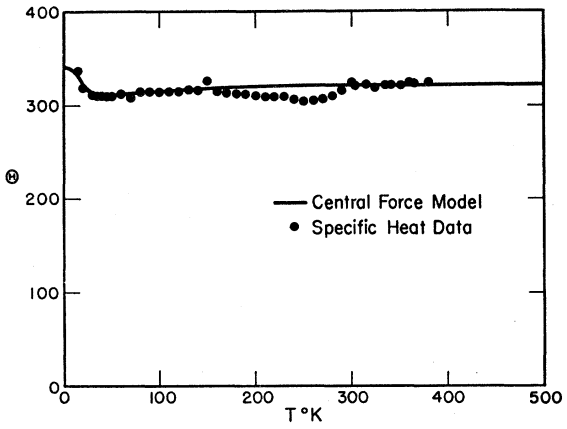

FIG. 5. The calculated and experimental effective specific heat Θ's.

TABLE I. Calculated effective x-ray Θ.

T(°K)	Θ(°K)
0	315
25	316
50	317
100	319
150	319
200	319
250	320
300	320
400	320
500	320

ACKNOWLEDGMENTS

The assistance of B. Veal and A. Singh in carrying out the x-ray measurements is gratefully acknowledged.

[9] W. F. Giauque and P. F. Meads, J. Am. Chem. Soc. **63**, 1897 (1941).
[10] H. L. Bronson, H. M. Chisholm, and S. M. Dockerty, Can. J. Research **8**, 282 (1933).
[11] B. N. Brockhouse and A. T. Stewart, Revs. Modern Phys. **30**, 236 (1958).
[12] D. R. Chipman, J. Appl. Phys. **31**, 2012 (1960); J. Boskovits *et al.*, Acta Cryst. **11**, 845 (1958).